University of North Carolina Asheville
Journal of Undergraduate Research
Asheville, North Carolina
December 2017

Dehydrogenation of Iridium (III) Sulfonamide Complexes

Cheryl Goldberg
Chemistry-General
The University of North Carolina Asheville
One University Heights
Asheville, North Carolina 28804 USA

Faculty Advisor: Dr. George Heard

Abstract

In this study seven Cp*Ir(pyridinesulfonamide)Cl precatalysts were geometrically optimized. A computational study of the energy of hydrogen removal from these seven catalytic species was able to identify the chain nitrogen (N1) as the site of protonation and transition states were predicted for both H_2 elimination and transfer hydrogenation reactions. Greater insight into the mechanism of these reactions was obtained and a characteristic energy for transfer hydrogenation was identified. The consistent relative energies of these transition state geometries suggest that the hydrogen removal step is not the rate limiting step of the reaction.

1. Introduction

Catalytic transfer hydrogenation has become an increasingly attractive alternative to traditional hydrogenation methods.[1] Transfer hydrogenation is characterized by the coupled oxidation of a hydrogen donor and reduction of a hydrogen acceptor.[1] As simple example of this time of reaction is $CH_2O + H_2 \rightarrow CH_3OH$. In the example reaction, formaldehyde is reduced to methanol. These reactions typically employ organometallic catalysts and are favorable due to the accessibility of safe and inexpensive hydrogen sources.[1,2,3,4]

In 2016, the O'Connor group at The College of New Jersey conducted transfer hydrogenation reactions using six Cp*Ir(pyridinesulfonamide)Cl precatalysts (Figure 1) which will heretofore be referred to as Species 1 through 7 (it should be noted that these species correspond to Species 5-11 in the O'Connor publication), seven acetophenone derivatives, and twelve substrates. It was found that electron rich precatalysts (Species 1, 3, 4, and 6) had the highest conversion rates when paired with electron poor substrates.[1] It was also found that when no substrate was provided and the reaction was heated, hydrogen gas was produced. Still unknown was the exact mechanism by which these reactions occurred, a question which this computational study seeks in part to answer. This study will focus on the second part of the process, how the protonated form of the catalyst is dehydrogenated. It is thought that Ir(III) coordinates with a hydride and a separate site on sulfonamide ligand is protonated however it is impossible to determine the protonation site experimentally which is why computational geometric optimization is necessary to identify the proper site. Once the ligand is protonated, the two hydrogens leave at the same time, either reducing a substrate or forming H_2 gas in the absence of a substrate.

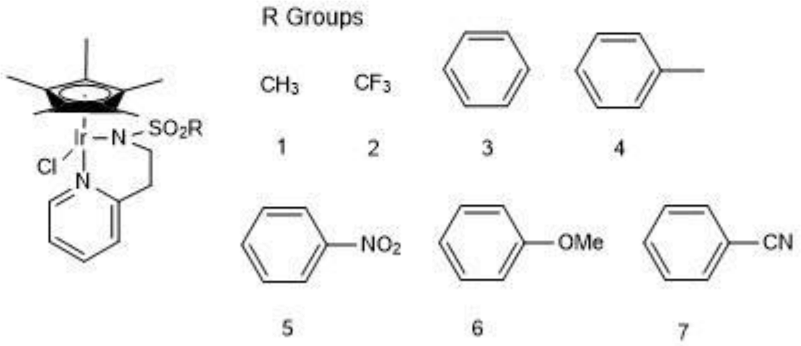

Figure 1. Library of Cp*Ir(pyridinesulfonamide)Cl precatalysts, species 1-7

2. Computational Methods

Calculations were performed using Gaussian 09 and Gaussian 16. The B3LYP[5,6] functional was used initially to get quick results and the geometries optimized by this method were used as starting points for M06[4,5,6] calculations with LANL2DZ[5,6,7] basis sets for iridium and 6-31g(d)[5,7] on all other atoms. LANL2DZ was used as a pseudopotential for iridium only.[5,6,7]

Geometric optimizations were obtained for all structures, and vibrational frequencies were calculated to ensure local minimum for each geometry. Transition state geometries were obtained by means of QST3 calculations.[4]

3. Results and Discussion

An analogous structure to those in presented Figure 1 was produced from a crystallographic image file received from the O’Connor group. This structure was used to determine the most effective basis set for this study. Geometric optimizations revealed a tetrahedral geometry.

Construction of Species 1-7 began after the publication of the experimental study. Geometries were optimized and transition states were characterized for all seven species but as all of the geometries are similar, Species 1 has been selected for discussion. The precatalytic species (Figure 2a) is a neutral 18 electron species and was found to have a tetrahedral geometry about the iridium atom. All important bond distances and angles for the Species 1 precatalyst structure were found to be within the range of experimental error for ORTEP data provided for the corresponding structure.[1] In order to become the catalytic species (Figure 2b), loss of the chloride is required resulting in a positively charged 16 electron species with a trigonal planar geometry. By coordinating the iridium atom to a hydrogen atom, a neutral hydride is formed with 18 electrons and a trigonal planar geometry (Figure 2c).

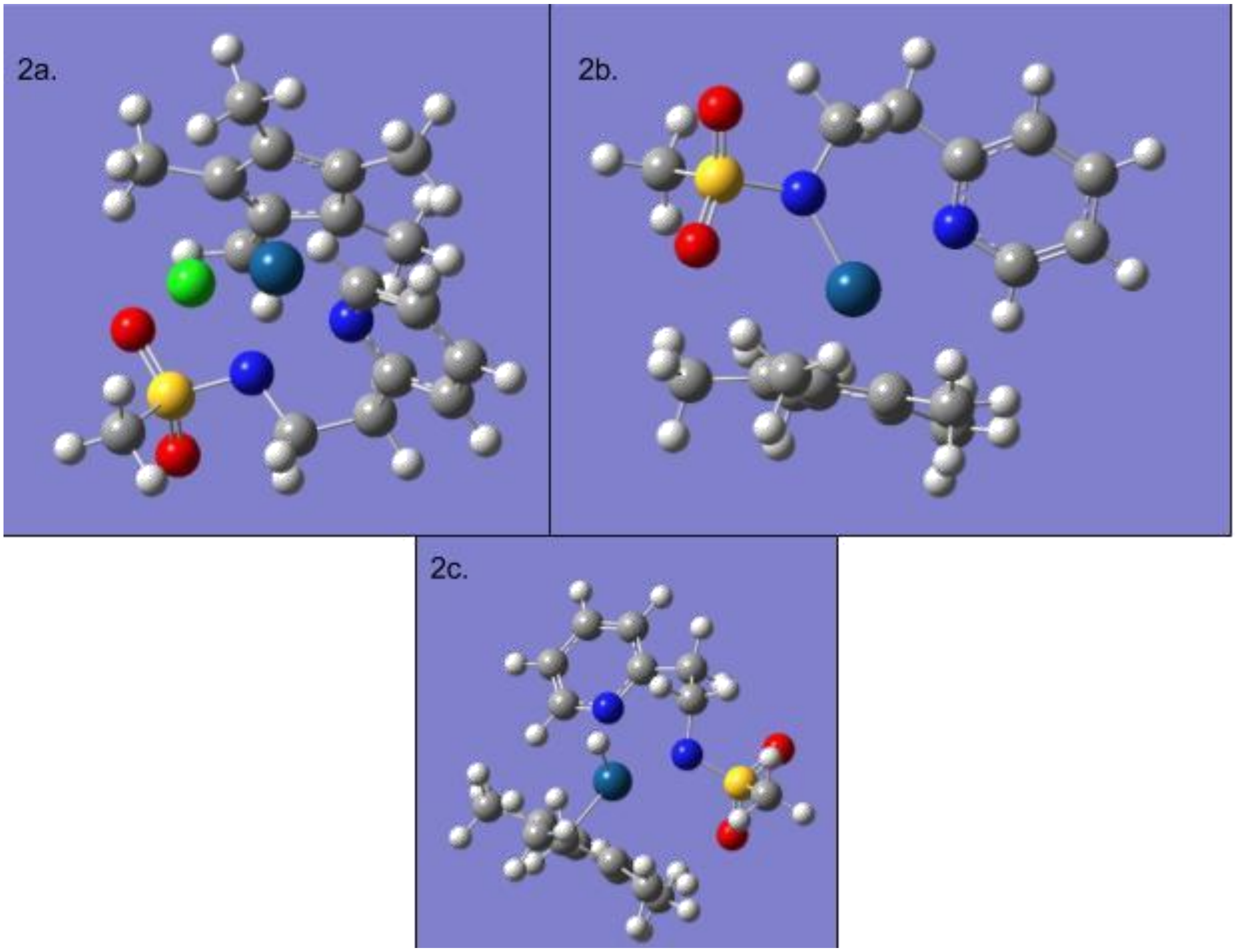

Figure 2. Precatalyst (a) Cation (b) and Hydride (c)

During their study of transfer hydrogenation, the O’Connor group found that when the reaction was heated and no substrate was provided, hydrogen gas was formed. Formation of hydrogen gas is indicative of concerted hydrogen removal and therefore the existence of a second site of hydrogen addition. It is thought that the hydrogen addition is concerted as well but at this time there is not enough information to support this assertion. To determine the most probable site of protonation, five structures with different protonation configurations were optimized (N1 (chain) cis to hydride, N1 trans to hydride, N2 (ring), O1 (closer to Ir), and O2). These structures can be found below as Figure 3a-e respectively. It was found that both the N1 trans and N2 configuration resulted in a trigonal planar structure with N2 no longer coordinated to Ir (Ir-N2 bond distances 4.03Å and 3.46Å respectively). The N1 (cis) protonation configuration was found to have the lowest energy of the five structures making it the most likely configuration. Based on the N1 (cis) energy, the difference in energy for each configuration was calculated. The difference in energy between N1 (cis) and N1 (trans) was found to be 94.34 kJ/mol. This large difference in energy can be attributed to the change in geometry undergone by the structure. Relative energies of the different protonation configurations can be found in Table 1. Important bond distances (in Angstroms) and bond angles for the relevant structures (Species 1) can be found in Table 2.

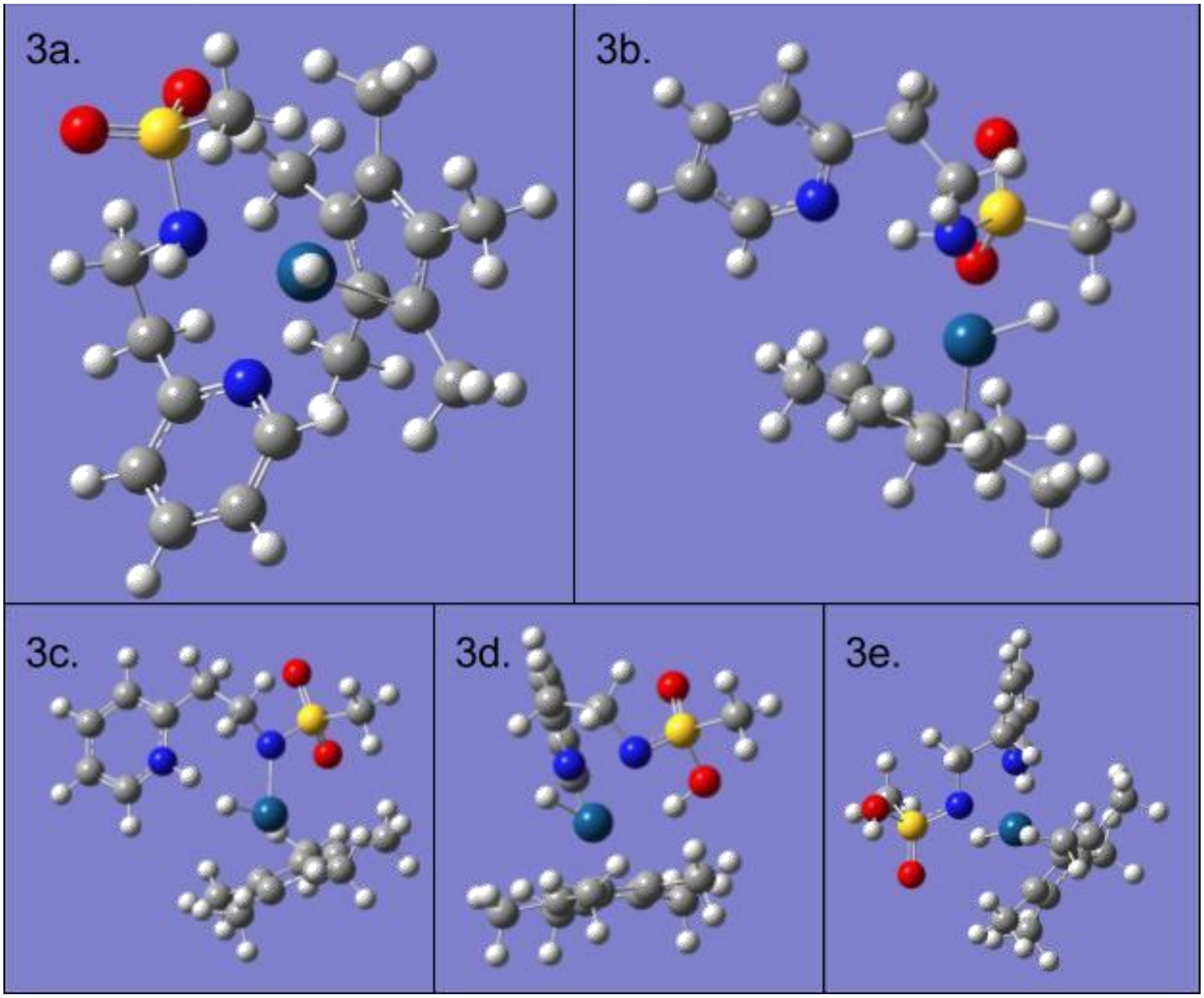

Figure 3. Different protonation configurations: N1 cis (a), N1 trans (b), N2 (c), O1 (d), O2 (e)

Table 1. Relative Energies (kJ/mol) of Varied Protonation Configurations (Species 1)

Protonation Site	Relative Energy (kJ/mol)
N1 (cis)	0
N1 (trans)	94.34
N2	74.79
O1	97.72
O2	68.88

Table 2. Important Bond Distances (Å) and Angles for Relevant Structures (Species 1)

	Precatalyst	Cation	Hydride	N1 (cis)	H_2 Elimination TS	Transfer Hydrogenation TS
Ir-Cl	2.46					
N1-Ir	2.11	1.97	2.12	2.24	2.24	2.11
N2-Ir	2.15	2.20	2.24	1.02	2.15	2.14
N1-Ir-N2	87.3°	86.6°	84.3°	77.7°	81.7°	81.0°
Ir-H			1.59	1.61	1.78	1.93
N1-H				1.02	1.45	1.14
H-H					0.97	2.07
O-Ir						3.00
O-H						1.12
C-H						1.57
C-N1						2.68

Once the protonation site had been determined, protonated hydride structures were optimized for all species. Calculations were run to isolate the transition state geometries and the relative energies for both H_2 elimination and transfer hydrogenation. Relative energies are necessary as each species has a different number of electrons; hence, comparing the raw energy data between different species provides no useful data. By subtracting the energy of the protonated hydride from the energy of the H_2 elimination transition state, the energy of the hydrogen removal could be estimated and these numbers could be compared between all seven species. To obtain the energy of removal for transfer hydrogenation, the energy of the substrate, formaldehyde (-114.4 Hartree), as well as the energy of the protonated hydride were subtracted from the transition state energy. All values were converted from Hartree to kJ/mol and are shown below (Table 3). Both the H_2 elimination transition state (4a) and the transfer hydrogenation transition state (4b) for Species 1 can be found in Figure 4.

Table 3. Energy of Removal for both H_2 Removal and Transfer Hydrogenation (kJ/mol)

Species	H_2 Removal	Transfer Hydrogenation
1	123.55	154.34
2	112.16	169.61
3	130.69	145.13
4	132.44	145.14
5	84.37	144.64
6	98.78	144.98
7	43.28	63.94

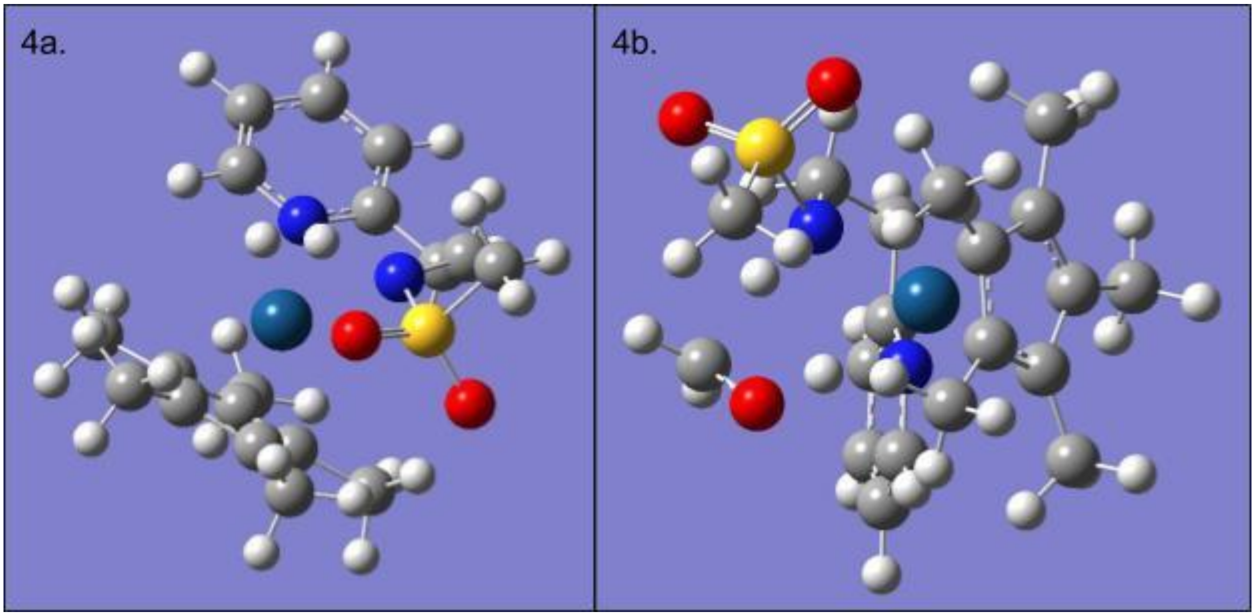

Figure 4. H_2 eliminations transition state (4a) and transfer hydrogenation transition state (4b) for Species 1

The energy of removal data is inconclusive in regard to identifying the most active species and shows no correlation between H_2 elimination and transfer hydrogenation activity. This indicates that this step of the reaction is not the rate determining step. There is little to be gleaned from the H_2 elimination energies with the exception of Species 7 which will be discussed (Species 1: 123.55 kJ/mol, Species 2: 112.16 kJ/mol, Species 3: 130.69 kJ/mol, Species 4: 132.44

kJ/mol, Species 5: 84.37 kJ/mol, Species 6: 98.78 kJ/mol, Species 7: 43.28 kJ/mol). The transfer hydrogenation energy numbers are slightly more telling (Species 1: 154.34 kJ/mol, Species 2: 169.61 kJ/mol, Species 3: 145.13 kJ/mol, Species 4: 145.14 kJ/mol, Species 5: 144.64 kJ/mol, Species 6: 144.98 kJ/mol, Species 7: 63.94 kJ/mol). The energies for Species 3-6 seem to indicate that there is a characteristic activation energy for transfer hydrogenation. Species 7 is shown to have the lowest activation energy which would lead one to the conclusion that Species 7 is clearly the most active catalytic species, however, experimental data does not back up that assertion. The low energy in this case might indicate a low affinity for hydrogen possibly making it the least active species.

The transition state geometries in Figure 4 show roughly the same N1-Ir-N2 bond angle (H_2 elim: 81.7°, TH: 81.0°) and the distances between Ir and the two nitrogens also shows no significant variance between the two structures (H_2 elim: N1-Ir 2.24Å, N2-Ir 2.15Å; TH: N1-Ir 2.11Å, N2-Ir 2.14Å). The distance between the hydrogen atoms is significant. The distance between hydrogen atoms is significant (H_2 elim: 0.97Å, TH: 2.07Å). These bond distances make sense as H_2 gas is the expected product in H_2 elimination. The average H-H bond distance is 0.75Å[8] and as this is a transition state, the atoms are in the process of coming together. The TH H-H bond distance does not indicate any interaction between the hydrogen atoms, these hydrogen atoms are in the process of leaving N1 and Ir and going to both ends of the formaldehyde carbonyl (H_2 elim: Ir-H 1.78Å, N1-H 1.45Å, TH: O-Ir 3.00Å, Ir-H 1.93Å, O-H 1.12Å, C-N1 2.68Å, N1-H 1.14Å, C-H 1.57Å). The N1-H distance in the protonated hydride is 1.02Å and the Ir-H distance is 1.61Å, these are shorter than the transition distances indicating the hydrogens moving from the sulfonamide and to the substrate.

3. Conclusion

Seven Cp*Ir(pyridinesulfonamide)Cl precatalysts were constructed and optimized using computational software and protonated hydride structures were identified. Transition states for both H_2 elimination and transfer hydrogenation were predicted and energies for hydrogen removal were calculated for each compound. These optimizations provided greater insight into the mechanisms of these reactions. It was initially the hope of the researcher that the relative energies of the transition states would line up with the experimental data and support the observation that Species 1, 3, 4, and 6 were the more active catalytic species however, the data was not conclusive with the possible exception of Species 7. The calculated energy barrier for Species 7 was found to be significantly lower than the energy barriers of the other six species for both hydrogen elimination and transfer hydrogenation condition. This very low activation energy likely indicates a very low affinity for H. This does support the experimental data. In light of the otherwise inconclusive data, it can be concluded that the hydrogen elimination step is not the rate limiting step for these reactions. The ultimate goal of this research is to determine the most probable mechanism for these reactions and in doing so, identify the most active species. There are other steps to consider in this reaction and so, work does and will continue.

4. Acknowledgements

The author would like to acknowledge Abby R. O’Connor, Benny C. Chan, George L. Heard, the UNCA Department of Chemistry, NSF grant CHE-1229406, Melody D. Goldberg, Corky Goldberg, and Phoebe Goldberg.

5. References

1. O’Connor, A. R. *Organometallics* **2016**, *35* (3), 327–335.
2. Wang, D.; Astruc, D. *Chemical Reviews* **2015**, *115*, 6621-6686.
3. Malacea, R.; Poli, R.; Manoury, E. *Coordination Chemistry Reviews* **2010**, *254*, 729-752.
4. Brieger, G. *Chemical Reviews* **1974**, *74*, 567-580.
5. Gaussian.com | Expanding the limits of computational chemistry http://www.gaussian.com
6. Schoenebeck, F. *Chemical Reviews* **2015**, *115*, 9532-9586.
7. Sunoj, R. *Chemistry - A European Journal* **2013**, *19*, 4069-4077.
8. Gilbert, T.; Kirss, R.; Foster, N.; Davies, G. *Chemistry*; Norton & Company: New York [u.a.], 2014.